Effect of canard stall on projectile roll and pitch damping

C Montalvo and M Costello

Proceedings of the Institution of Mechanical Engineers, Part G: Journal of Aerospace Engineering published online 4 July 2011
DOI: 10.1177/0954410011403578

Effect of canard stall on projectile roll and pitch damping

C Montalvo and **M Costello***
School of Aerospace Engineering, Georgia Institute of Technology, Atlanta, Georgia, USA

The manuscript was received on 30 August 2010 and was accepted after revision for publication on 21 February 2011.

DOI: 10.1177/0954410011403578

Abstract: A computational and mathematical approach is used to investigate the effect of canard stall on projectile roll and pitch damping. For spinning projectiles with dithering canards, large angles of attack can be achieved by these canards. These large angles of attack can lead to stall that causes abnormal loads on the projectile. Because of these abnormalities, it is important to include the effects of stall on the projectile. First, the total roll and pitch moments of two canards is derived. These equations are then analysed to show that the effects of canard stall can produce a decrease in roll damping, causing roll rate to increase, and an increase in pitch damping, causing the no roll frame pitch rate to decrease. To validate this analysis, simulation is performed using a fully non-linear six-degree-of-freedom dynamic model with canard aerodynamics. The results from the simulation agree with the equations derived; thus, for projectiles that use dithering canards for control, it is important to include these non-linear effects in the projectile dynamic model.

Keywords: projectiles, canards, control, stall

1 INTRODUCTION

Canards are a common control mechanism used in smart projectiles that provide manoeuvre capability and range extension [**1**–**4**]. Typically, relatively small canards mounted on the front of the projectile provide sufficient control authority to enable accurate flight control. Deployed canards create changes in the overall aerodynamic characteristics of the body, most notably increased drag. Deployed canards also affect the aerodynamic roll and pitch damping. For rolling, fin-stabilized projectiles, canard deflection angle is dithered in an oscillatory fashion to create inertial fine trajectory changes. The amplitude of canard angle dithering is a key design variable as is canard area [**5**]. Given physical real-estate constraints for practical systems, canard area is typically set relatively low with dither angles set fairly high to achieve acceptable manoeuvrability. When combining projectile spin and body motion with canard dithering, it is often the case that canards stall over some portion of their roll cycle. Although much has been accomplished in formulation of control algorithms for said canard-controlled projectiles [**3**, **4**], stall effects have not been included. Moreover, canard stall effects on projectile dynamics are not well understood. The purpose of this article is to examine the effect of canard stall on roll and pitch damping characteristics and resulting roll and pitch response. Using analysis and simulation, it is shown that during stall, the effect of canards on roll and pitch damping of the projectile is modified with the key controlling variable being the canard lift curve slope. In stall, roll damping is decreased, leading to a high spin rate, while pitch damping is increased, leading to significant changes in angular rate response. Thus, for canard-controlled projectiles with large dither amplitudes or body angular motion, it is important to include these effects in analysis.

**Corresponding author: School of Aerospace Engineering, Georgia Institute of Technology, Atlanta, GA 30332, USA.*
email: mark.costello@ae.gatech.edu

2 DYNAMIC MODELLING

To consider canard stall effects on a spinning projectile, a standard projectile flight dynamic modelling

approach is employed. The 12 equations of motion describing the flight dynamics of the projectile are given below in equations (1) through (4). These equations are well known and reported in many sources [**6**]

$$\begin{Bmatrix} \dot{x} \\ \dot{y} \\ \dot{z} \end{Bmatrix} = \begin{bmatrix} c_\theta c_\psi & s_\phi s_\theta c_\psi - c_\phi s_\psi & c_\phi s_\theta c_\psi + s_\phi s_\psi \\ c_\theta s_\psi & s_\phi s_\theta s_\psi + c_\phi c_\psi & c_\phi s_\theta s_\psi - s_\phi c_\psi \\ -s_\theta & s_\phi c_\theta & c_\phi c_\theta \end{bmatrix} \begin{Bmatrix} u \\ v \\ w \end{Bmatrix} \tag{1}$$

$$\begin{Bmatrix} \dot{\phi} \\ \dot{\theta} \\ \dot{\psi} \end{Bmatrix} = \begin{bmatrix} 1 & s_\phi t_\theta & c_\phi t_\theta \\ 0 & c_\phi & -s_\phi \\ 0 & s_\phi / c_\theta & c_\phi / c_\theta \end{bmatrix} \begin{Bmatrix} p \\ q \\ r \end{Bmatrix} \tag{2}$$

$$\begin{Bmatrix} \dot{u} \\ \dot{v} \\ \dot{w} \end{Bmatrix} = \begin{Bmatrix} X/m \\ Y/m \\ Z/m \end{Bmatrix} - \begin{bmatrix} 0 & -r & q \\ r & 0 & -p \\ -q & p & 0 \end{bmatrix} \begin{Bmatrix} u \\ v \\ w \end{Bmatrix} \tag{3}$$

$$\begin{Bmatrix} \dot{p} \\ \dot{q} \\ \dot{r} \end{Bmatrix} = \begin{bmatrix} I_{xx} & I_{xy} & I_{xz} \\ I_{xy} & I_{yy} & I_{yz} \\ I_{xz} & I_{yz} & I_{zz} \end{bmatrix}^{-1} \left[\begin{Bmatrix} L \\ M \\ N \end{Bmatrix} - \begin{bmatrix} 0 & -r & q \\ r & 0 & -p \\ -q & p & 0 \end{bmatrix} \begin{bmatrix} I_{xx} & I_{xy} & I_{xz} \\ I_{xy} & I_{yy} & I_{yz} \\ I_{xz} & I_{yz} & I_{zz} \end{bmatrix} \begin{Bmatrix} p \\ q \\ r \end{Bmatrix} \right] \tag{4}$$

The applied forces and moments in equations (3) and (4) contain contributions from the weight of the projectile, body aerodynamic forces, and canards [**5**].

The aerodynamic force due to a single canard is modelled as a point force acting at the lifting surface aerodynamic centre, as shown in Fig. 1. The orientation of a particular canard is obtained by one body-fixed rotation. Starting with the canard axis aligned with the projectile body axis, the canard is rotated about the $\vec{I}_B$ axis by the azimuthal (ϕ_{C_i}) angle. Figure 2 shows a diagram of the two canards used in this development. Strip theory is used to compute the canard aerodynamic loads [**6**]. Notice in Fig. 1 that the aerodynamic angle of attack of the ith canard is calculated using only the u_{AC_i} and w_{AC_i} components of the relative air velocity experienced by the canard computation point. In the projectile body axis, the ith canard force is given by equation (5). The transformation matrix T_{C_i} is shown in equation (6).

$$\begin{Bmatrix} X_{C_i} \\ Y_{C_i} \\ Z_{C_i} \end{Bmatrix} = q_{C_i} S_{C_i} [T_{C_i}] \begin{Bmatrix} C_{L_{C_i}} \sin(\alpha_{C_i} - \delta_i) - C_{D_{C_i}} \cos(\alpha_{C_i} - \delta_i) \\ 0 \\ -C_{L_{C_i}} \cos(\alpha_{C_i} - \delta_i) - C_{D_{C_i}} \sin(\alpha_{C_i} - \delta_i) \end{Bmatrix} \tag{5}$$

$$T_{C_i} = \begin{bmatrix} 1 & 0 & 0 \\ 0 & \cos(\phi_{C_i}) & -\sin(\phi_{C_i}) \\ 0 & \sin(\phi_{C_i}) & \cos(\phi_{C_i}) \end{bmatrix} \tag{6}$$

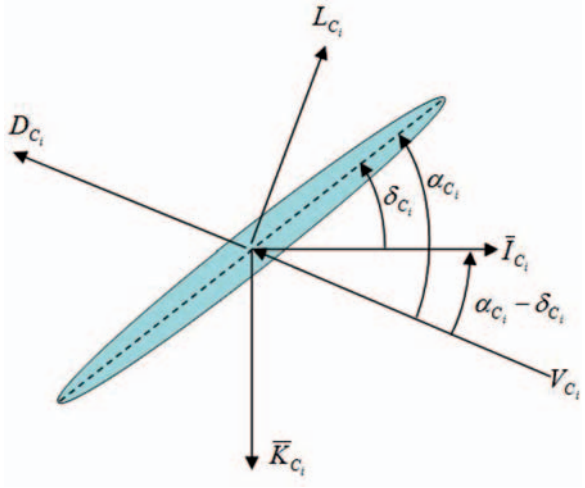

Fig. 1 Canard aerodynamic model force diagram

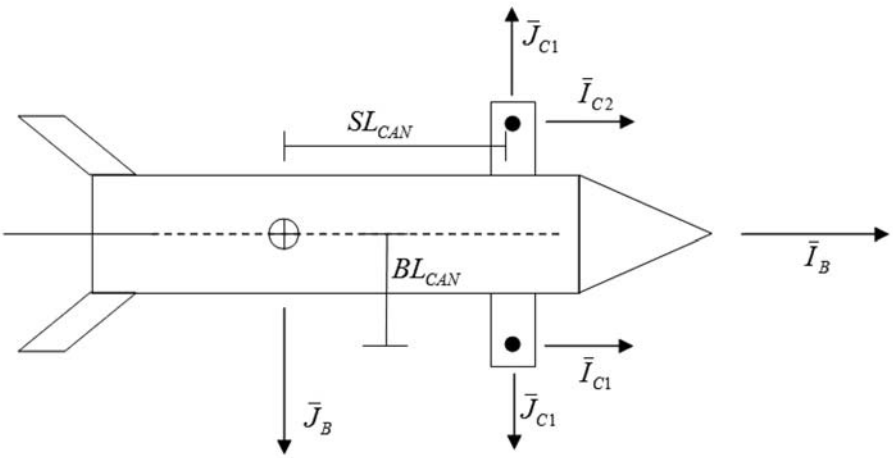

Fig. 2 Projectile model with canards

In equation (5), q_{C_i} is the dynamic pressure at the canard computation point, S_{C_i} the canard reference area, and δ_i the canard deflection angle. Dynamic pressure is given by equation (7)

$$q_{C_i} = \frac{1}{2}\rho\left(u^2_{A_{C_i}} + v^2_{A_{C_i}} + w^2_{A_{C_i}}\right) \tag{7}$$

The canard lift and drag coefficients are linearly expanded terms of canard aerodynamic angle of attack and local Mach number at the canard computation point. Finally, the angle of attack of the canard is computed using the equation below

$$\alpha_{C_i} = \tan^{-1}\left(\frac{w_{A_{C_i}}}{u_{A_{C_i}}}\right) + \delta_i \tag{8}$$

3 ROLL AND PITCH DAMPING ANALYSIS

To analyse pitch and roll damping effects of the canards, Fig. 2 is used as an aid to generate expressions for the total roll moment. The rotation angle for canard 1 is zero and canard 2 has an azimuthal angle equal to π. The roll moment of each canard is computed by calculating the normal force at each canard and then multiplying this by the distance from the centre-line of the projectile to the canard computation point, BL_{CAN}.To compute the dynamic pressure at the canards, the equation relating two points on a rigid body is used [**6**]. The velocities for canard 1 are shown below. The velocities at canard 2 can be obtained in a similar fashion. The SL_{CAN} parameter is the distance along the I_B axis from the centre of gravity of the projectile to the canard computation point.

$$\left\{\begin{array}{c} u_{A_{C1}} \\ v_{A_{C1}} \\ w_{A_{C1}} \end{array}\right\} = \left\{\begin{array}{c} u - rBL_{CAN} \\ v + rSL_{CAN} \\ w - qSL_{CAN} + pBL_{CAN} \end{array}\right\} \tag{9}$$

To form a compact final expression for the roll moment, it is assumed that the total velocity experienced by both canards is the same, $V_{A_{C1}} \approx V_{A_{C2}}$. Although the canards experience large differences in angle of attack, the total velocity on both canards is roughly the same since the yaw and pitch rates are relatively small. The general equation for lift is shown below

$$C_{L_i} = C_{L_0} + C_{L\alpha_C}\alpha_{C_i} \tag{10}$$

Finally, the angle of attack of the canards is assumed small such that the angle of attack can be approximated as $\alpha_{C_i} \approx \frac{w_{A_{C_i}}}{V_A} + \delta_i$. The total roll moment only due to the canards then reduces to equation (11), where $\delta_C = \delta_1 = -\delta_2$

$$\begin{aligned} L_C &= q_L\left[C_{L\alpha_C}BL_{CAN}\left(r\delta_C - \frac{pu}{V_A} + \frac{r(w - qSL_{CAN})}{V_A}\right)\right. \\ &\quad \left. - pBL_{CAN}C_{D0} - C_{L0}u\right] \\ q_L &= \rho V_A S_C BL_{CAN} \end{aligned} \tag{11}$$

The dominant terms in the equation above are the terms involving the roll rate of the projectile. These are standard roll damping terms. The roll rate of the projectile is so large compared to the pitch and yaw rates that the total roll moment creates significant roll damping on the projectile. The other terms are relatively small even for a controlled trajectory.

An interesting point to note is that if the canards stall so that $C_{L\alpha_C}$ switches sign, the largest roll damping term becomes positive and actually creates a roll rate increase. Furthermore, the term $r\delta_C$ is extremely small since the canard deflection angle maximum is

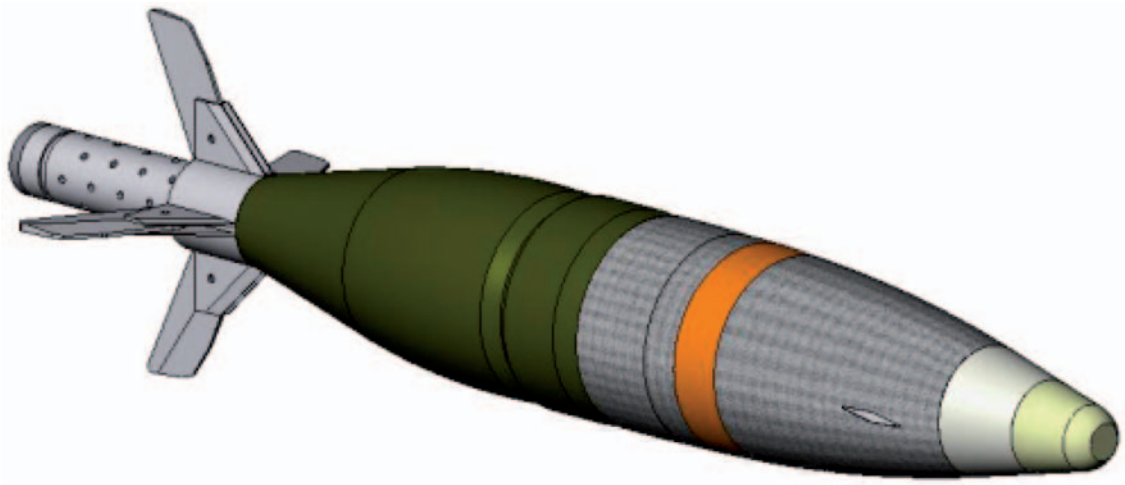

Fig. 3 Example of fin-stabilized projectile with canards retracted

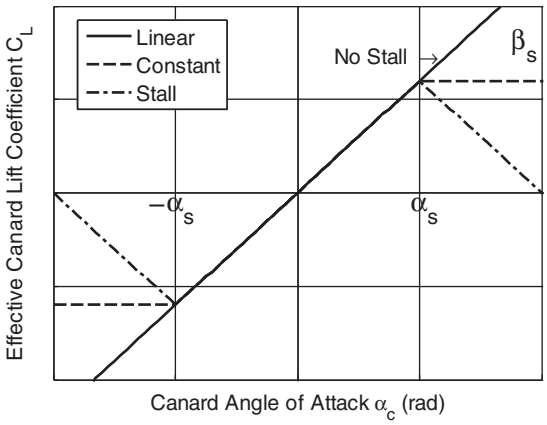

Fig. 4 Lift curve models

Table 1. Initial conditions for simulation

Position (ft)	Attitude (rad)	Velocity (m/s)	Attitude rates (rad/s)
$x=0$	$\phi=0$	$u=294.07$	$p=0$
$y=0$	$\theta=1.08$	$v=0$	$q=0$
$z=0$	$\psi=0$	$w=0$	$r=0$

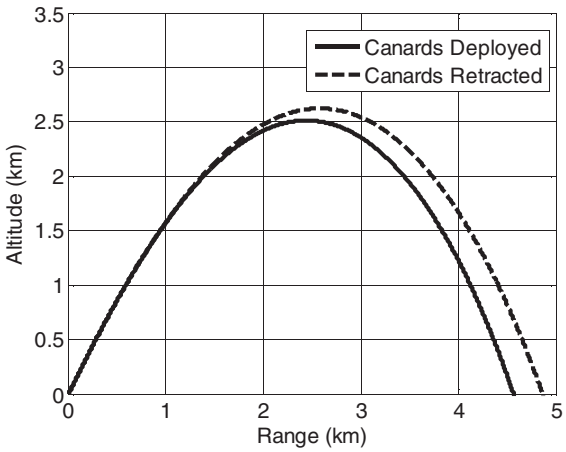

Fig. 5 Ballistic trajectory – altitude versus range

only about 15° or 0.25 radians. Thus, when the canards start to dither, there should be almost no change in the roll moment produced by the canards assuming that the angle of attack of the canards stays within the linear regime of the lift curve slope.

The total pitch moment of the canards can be found in a similar way as the roll moment. The equation for total canard pitch moment is shown below

$$M_C = q_M\left[C_{L\alpha_C}\left(u\delta_C + \frac{W_q u - prBL_{CAN}^2}{V}\right) + W_q C_{D0} - rBL_{CAN}C_{L0}\right]$$
$$q_M = \rho V_A S_C SL_{CAN}. W_q = w - qSL_{CAN} \quad (12)$$

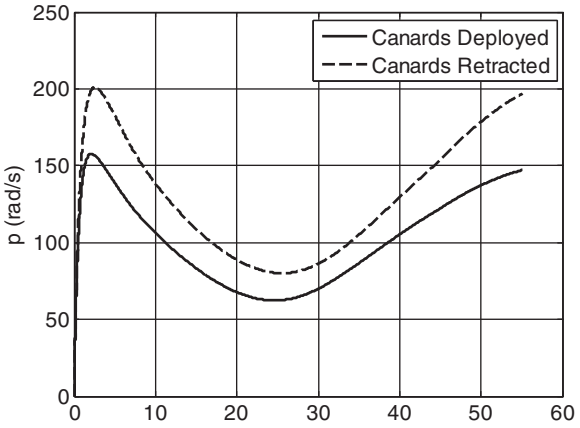

Fig. 6 Ballistic roll rate versus time

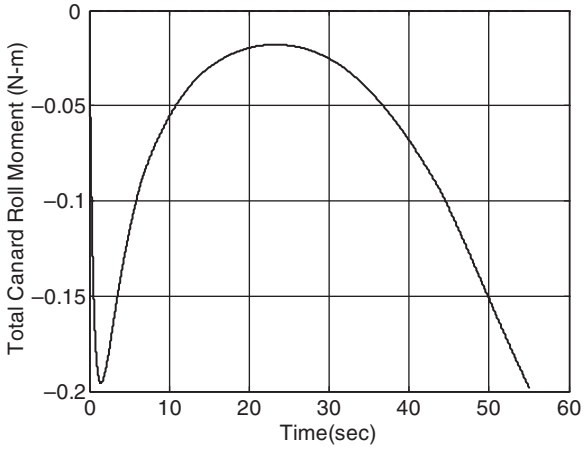

Fig. 7 Ballistic roll moment versus time

The equation above shows a strong dependence on canard deflection angle since it is multiplied by the forward velocity of the projectile. Thus, the pitching moment increases when canards are dithered. In stall, when the lift curve is negative, the average moment per roll cycle decreases.

4 RESULTS

To verify the simple equations above, trajectory results for a sample projectile are generated for different dithering canard scenarios, including cases where the canards are stalled over a portion of the roll cycle. An industry standard fully non-linear six-degree-of-freedom simulation tool called BOOM is employed for these purposes [**7**]. The projectile used is shown in Fig. 3. This projectile is fin stabilized, 5 kg and is 0.61 m in length. The projectile uses two forward canards that dither to a maximum deflection of 15°. The canards are positioned 0.13 m forward of the centre of gravity with a canard area of 12.08 cm^2. The lift curve of the canards is modelled as linear between

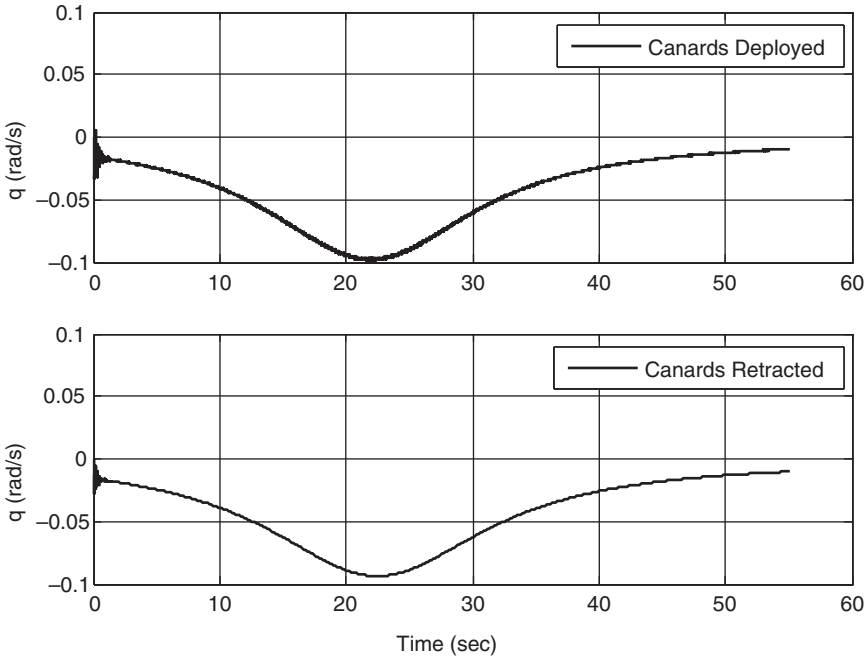

Fig. 8 Ballistic pitch rate (no roll frame) versus time

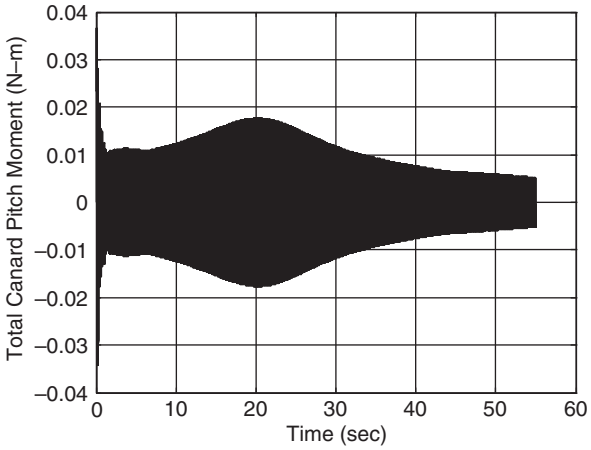

Fig. 9 Ballistic pitch moment versus time

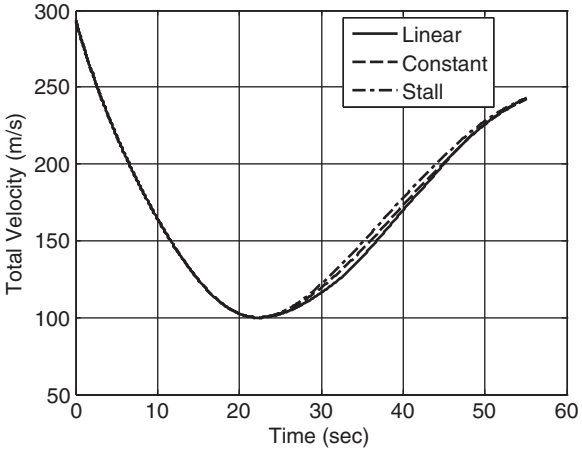

Fig. 11 Controlled velocity versus time

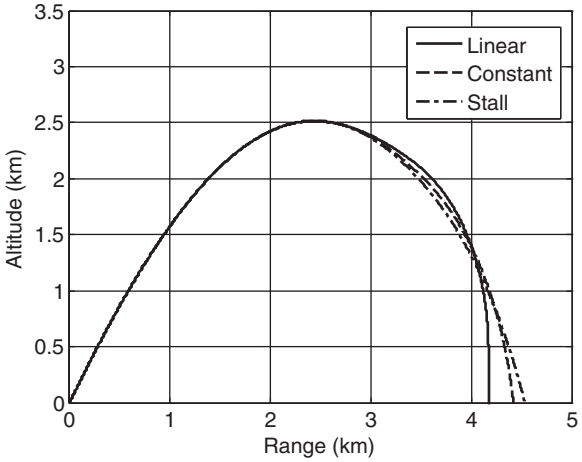

Fig. 10 Controlled trajectory – altitude versus range

a certain angle of attack range and then stalled outside of this range. Figure 4 depicts the lift coefficient representation. Notice that the simple stall model is fully specified by β_S and α_S. For verification purposes and to match the data for this projectile, α_S is set at 10° and β_S is set at 0°, 45°, and 90°. The three scenarios are called linear, constant, and stall, respectively. The initial conditions for the simulated trajectories are shown in Table 1.

To analyse the effects of the canards without any control, the canard deflection angle is first set to zero. Two trajectories are simulated, one with the canards deployed and the other with the canards retracted. Since this is a ballistic trajectory, the angle of attack of the canards remains in the linear regime. Figure 5

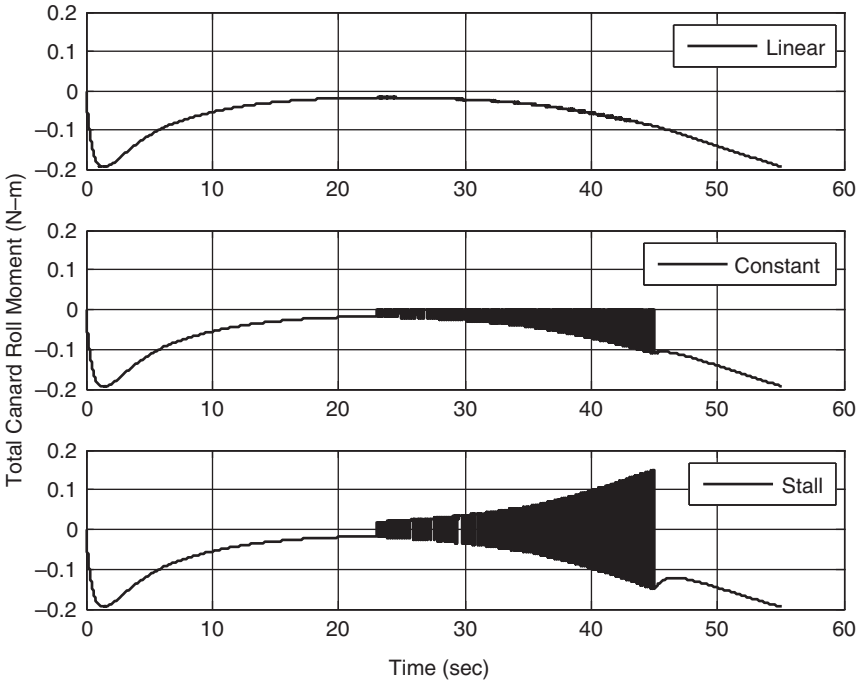

Fig. 12 Total canard roll moment versus time

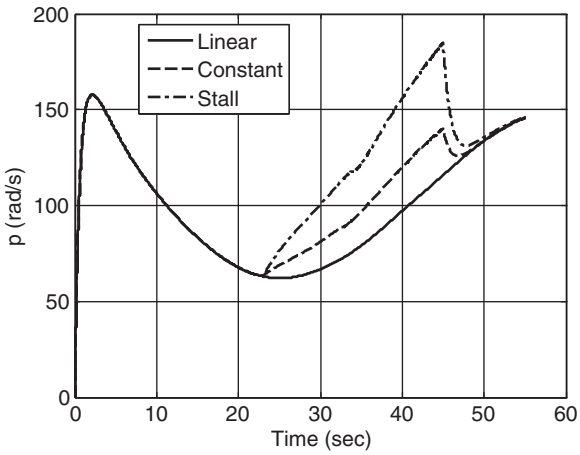

Fig. 13 Controlled roll rate versus time

shows the altitude versus range for the two trajectories. When the canards are deployed, they create more drag on the projectile and range is reduced. Figure 6 shows roll rate which is lower when the canards are deployed because of the two dominant roll damping terms found in equation (11). The total roll moment is negative throughout the duration of the flight, as depicted in Fig. 7. Just as the simple equation predicts, the pitch rate remains quite similar, as seen in Fig. 8 which shows the pitch rate in the no roll frame to decrease ambiguity. In addition, the pitch moment which only oscillates between about 0.014 N-m is very small, as shown in Fig. 9.

To investigate the effect of canard stall, the dither angle is set so that the canard is stalled over a portion of the roll cycle. To do this, a model predictive controller is used to command the projectile to a range of about 4.2 km. The control system is activated at 23 s into the flight which corresponds to the apogee of the flight and promptly deactivated at 45 s. Figure 10 shows the trajectory for all three β_S angles. The linear model reaches the target location since it has the most canard effectiveness. The other two trajectories incorporate a loss in lift when the angle of attack of the canards is larger than α_S. An important note to make is that the overall velocity of the projectile remains quite similar for all three trajectories, as shown in Fig. 11.

The equations derived previously predict that the roll moment increases when the canards stall and cause the roll rate to increase. Figure 12 shows that the total canard roll moment changes negligibly for the linear case, becomes zero at times for the constant case, and even becomes positive for the stall case. Thus, as shown in Fig. 13, the roll rate using the linear model remains unchanged but when the stall model is incorporated, the roll rate increases considerably. In addition, when the control system is deactivated, the roll moment and roll rate returns to the value of the linear case. Just as the pitch moment equation predicts, the pitch moment decreases when the stall model is used and as such increases pitch damping, causing the pitch rate to

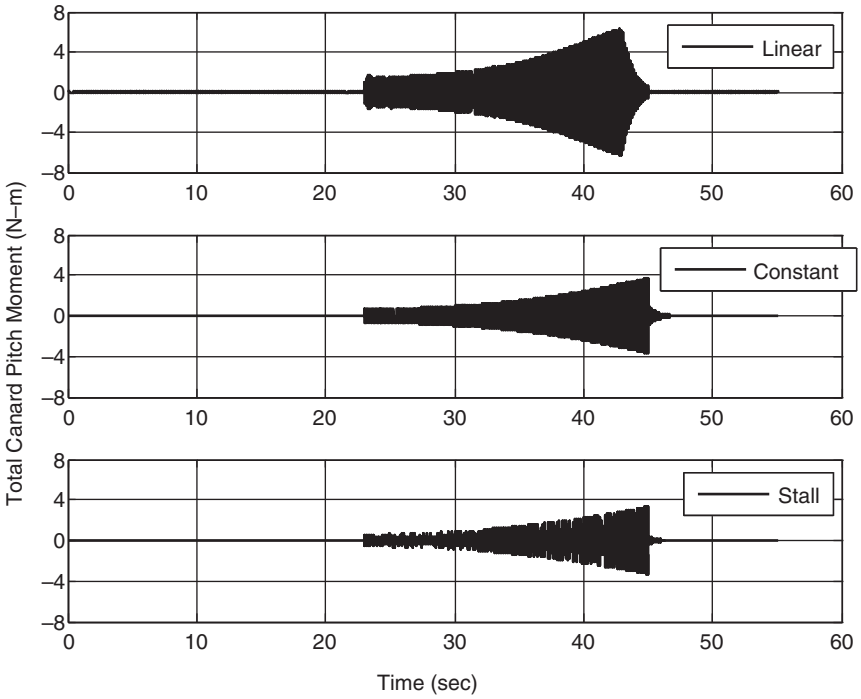

Fig. 14 Total canard pitch moment versus time

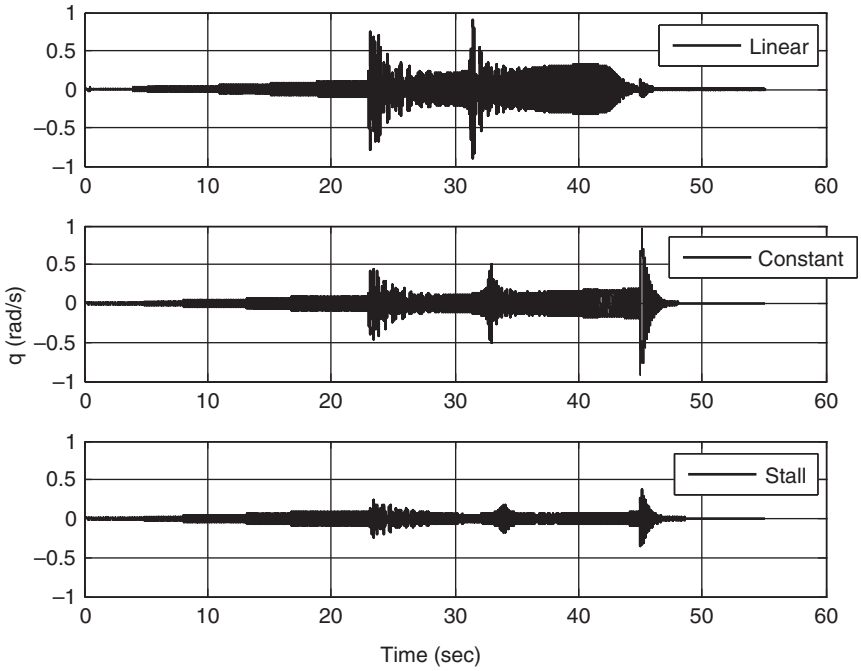

Fig. 15 Controlled pitch rate versus time

decline. Figure 14 shows the total canard pitch moment and Fig. 15 the pitch rate declining as a function of β_S. When the control system is deactivated the pitch moment increases and causes the pitch rate to spike. Note that in the linear case, the pitch moment of the canards increases by more than 500 times the ballistic simulation which is caused by the first term in the pitch moment equation. Due to the increase in pitch damping and loss of canard effectiveness, it is also clear that the body angle of attack, shown in Fig. 16, and the canard angle of attack, Fig. 17, decreases as a function of β_S.

5 CONCLUSIONS

When modelling spinning, fin-stabilized, canard-controlled projectiles, it is important to fully model the lift on the canards. If the canards reach a point where they stall over a portion of the roll cycle, the canards lose their damping effectiveness. This effect can be particularly important for some projectile configurations where specific roll rate characteristics are an integral part of the overall operation of the munition. Simple expressions were developed that clearly explain how canard stall affects angular rate damping of the round. These expressions should prove useful to smart projectile designers in sizing controllable canards.

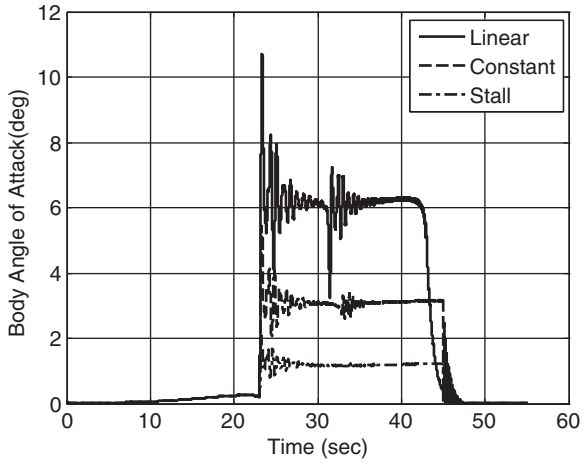

Fig. 16 Body angle of attack versus time

REFERENCES

1 **Costello, M.** Range extension and accuracy improvement of artillery projectiles. In *Proceedings of the 1995 AIAA atmospheric flight mechanics conference,* American Institute of Aeronautics and Astronautics, 7–9 August 1995, Baltimore, Maryland, paper no. 97-3724.

2 **Costello, M.** Extended range of a gun launched smart projectile using controllable canards. *Shock Vib.*, 2001, **8**(3–4), 203–213.

3 **Rogers, J.** and **Costello, M.** Design of a roll-stabilized mortar projectile with reciprocating canards. *J Guid. Contr. Dynam.*, 2010, **33**(4), 1026–1034.

4 **Ollerenshaw, D.** and **Costello, M.** Model predictive control of a direct fire projectile equipped with canards, 2005, Proceedings of *AIAA atmospheric flight mechanics conference and exhibit*, 15–18 August, San Francisco, California, paper no. 2005-5818.

5 **McCoy, R.** *Modern exterior ballistics: the launch and flight dynamics of symmetric projectiles*, 1998 (Schiffer Publishing, Ltd, Atglen, Pennsylvania).

6 **Etkins, B.** *Dynamics of atmospheric flight*, 2000 (Dover Publications, Mineola, New York).

7 **Costello, M.** and **Anderson, D.** Effect of internal mass unbalance on the terminal accuracy and stability of a projectile. In *Proceedings of the 1996 AIAA flight mechanics conference*, 29–31 July 1996, San Diego, California, paper no. 96-3447 .

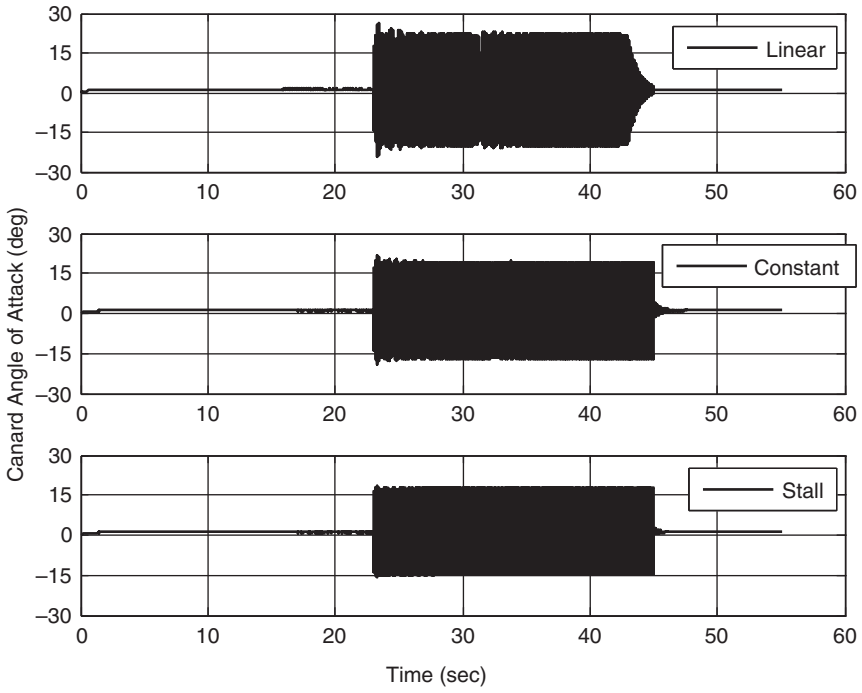

Fig. 17 Canard angle of attack versus time

APPENDIX

Notation

$C_{L\alpha}$	lift curve slope of the canards
C_{L0}, C_{D0}	zero angle of attack force coefficients
C_{LC_i}, C_{DC_i}	aerodynamic force coefficients of ith canard
I_{xx}, I_{yy}, I_{zz}, I_{xz}, I_{yz}, I_{xy}	projectile moments of inertia in body reference frame
L, M, N	components of external moments acting on projectile in body reference frame
L_{C_i}, M_{C_i}, N_{C_i}	components of external moments created by the ith canard in body reference frame
p, q, r	components of angular velocity vector in body reference frame
q_{C_i}	dynamic pressure at the ith canard
S_{C_i}	reference area of ith canard
SL_{CAN}, BL_{CAN}	distance from mass centre to canard computation point
T_{C_i}	transformation matrix from the ith canard reference frame to body reference frame
u, v, w	components of velocity vector of mass centre in body reference frame
u_{AC_i}, v_{AC_i}, w_{AC_i}	aerodynamic velocity components at canard computation point in body reference frame
V_{A_i}	total aerodynamic velocity of ith canard
x, y, z	components of position vector of mass centre in an inertial frame
X, Y, Z	components of external forces acting on projectile in body reference frame
X_{C_i}, Y_{C_i}, Z_{C_i}	components of external forces created by the ith canard in body reference frame
α_{C_i}	aerodynamic angle of attack of ith canard
α_S, β_S	lift curve slope model parameters
δ_{C_i}	ith canard deflection angle
ρ	air density
ϕ, θ, ψ	Euler roll, pitch, and yaw angles of projectile
ϕ_{C_i}	rotation angle of the ith canard about the $\vec{I}_B$ body axis